THE JOURNAL OF PHYSICAL CHEMISTRY C

ARTICLE

pubs.acs.org/JPCC

Adsorption and Separation of CO_2/CH_4 on Amorphous Silica Molecular Sieve

Kunimitsu Morishige

Department of Chemistry, Okayama University of Science, 1-1 Ridai-cho, Kita-ku, Okayama 700-0005, Japan

Supporting Information

ABSTRACT: Adsorption and separation of CO_2/CH_4 were examined on two kinds of amorphous silica molecular sieves, ASMS-3A and ASMS-5A, that are composed of spherical cavities arranged in a face-centered-cubic array and connected through narrow necks of molecular dimensions. For ASMS-3A, the exclusion of CH_4 molecules due to their dimensions into the narrow necks and preferential adsorption of CO_2 with the smaller kinetic diameter is observed at 283 K. In addition, the amount of CO_2 adsorbed at 283 K does not decrease at all with surface hydration. All these results suggest that ASMS-3A is a promising candidate for the separation and purification of CO_2 from various CO_2/CH_4 mixtures such as natural gas and landfill gas by a PSA process.

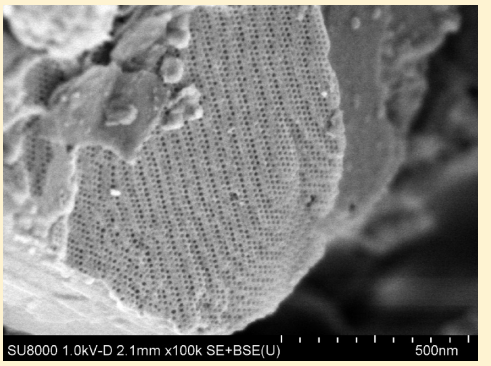

I. INTRODUCTION

Removal of carbon dioxide from natural gas is an important process in upgrading the gas.[1,2] CO_2 is often found as an impurity in natural gas, where methane is the major component. The presence of CO_2 reduces the energy content of natural gas and can lead to pipeline corrosion in the presence of water. For the removal of CO_2, several technologies, such as absorption, cryogenic distillation, membrane separation, and adsorption, have been used. Among these, adsorption in porous materials is energetically efficient and economically competitive, especially for the case of medium and small volumes of gas to be processed.[2,3] Pressure swing adsorption (PSA) is one of the most known industrial processes for gas separation.[4] The PSA process is based on the selective adsorption of one component of a gas mixture at relatively high pressures and its release upon decreasing pressure.

A key step in the design of PSA processes for the separation and purification of CO_2 is the selection of a highly selective adsorbent with a high CO_2 capacity. However, it is also necessary that the affinity of the adsorbent to CO_2 is not too high because otherwise the regeneration step can negatively affect the economy of the process. Most studies of CO_2/CH_4 separation have focused on zeolites,[5−19] carbon-based adsorbents,[20−26] and metal−organic framework (MOFs).[27−47] Zeolites of low Si/Al ratios exhibit very high selectivity of CO_2 adsorption over CH_4 at low pressures, although the selectivity rapidly decreases with an increase of pressure over a pressure range where a PSA process is actually operated. The high selectivity usually results in the poor regenerability of the adsorbents. Regenerability of the adsorbent can be remarkably improved by using the siliceous form of zeolite, although the high selectivity is lost.[18] Generally speaking, specific interactions of adsorbed CO_2 molecules with the surfaces increase the selectivity of CO_2 adsorption over CH_4 while reducing the regenerability of the adsorbents. For the application of the PSA process, a molecular sieve separation of CO_2 from CH_4 owing to the smaller kinetic diameter of former molecule than the latter would be more suitable than the separation based on the different adsorption affinities. Carbons generally exhibit better adsorbent regenerability compared to zeolites. However, the CO_2/CH_4 selectivities on carbons are not so good as zeolites. Some kinds of MOFs exhibit high adsorption capacities of CO_2 and/or high selectivities for CO_2 separation from CO_2/CH_4 mixtures under the usual working conditions of the PSA process. However, thermal and mechanical stabilities of MOFs are inferior to zeolites and carbons. The development of adsorbents with a high CO_2 capacity, good CO_2/CH_4 selectivity, excellent regeneration properties, and high thermal and mechanical stabilities is of paramount importance in natural gas upgrading by the PSA process.

Very recently, we have discovered that the ordered large-pore cagelike silicas prepared without and with the hydrothermal treatment at low temperatures show a molecular sieving effect for simple gases such as carbon dioxide and nitrogen depending on the hydrothermal treatment conditions.[48] The effect seems to indicate that the materials possess necks of molecular dimensions as a result of the templating of the spherical copolymer micelles bridged by the single poly(ethylene oxide) chains. Because the ordered silicas are not crystalline in their atomic arrangement, however, this does not necessarily indicate that the necks in the

Received: March 18, 2011
Revised: April 15, 2011
Published: April 27, 2011

material are uniform in size. In the ordered silicas with cagelike pores, almost spherical cavities are arranged in a three-dimensional (3D) lattice and connected through narrow necks.[49] All the cavities are of almost the same size, whereas the necks possess a finite size distribution inherent to the ordered silicas with cagelike pores.[50,51] The molecular sieving properties of the materials seem to be well accounted for by the bond-controlled percolation of a gas in the interconnected cavities.[48] The neck size available for the molecular sieving can be effectively tailored by properly adjusting the conditions of the hydrothermal treatment. This feature makes the large-pore cagelike silica with necks of molecular dimensions promising candidates for a new type of molecular sieves.

In this work, we measured the adsorption−desorption isotherms of CO_2, CH_4, N_2, and O_2 on two kinds of amorphous silica molecular sieves (ASMSs) at 283 K for pressures up to 10 atm. Adsorption and separation of CO_2/CH_4 mixture was predicted using the ideal adsorbed solution theory (IAST)[52] from the single-component CO_2 and CH_4 isotherms. In industrial processes, contamination of adsorbents with moisture is easy to occur because all gases contain some moisture under practical conditions. In order to examine the effect of adsorbed water on the adsorption properties of these materials, we further measured the adsorption−desorption isotherms of CO_2 at 283 K and H_2 and N_2 at 77 K on the samples before and after surface hydration.

II. EXPERIMENTAL SECTION

1. Materials and Characterization. Two kinds of amorphous silica molecular sieves (ASMS-3A and ASMS-5A) were prepared by using Pluronic F127 triblock copolymer as a structure-directing agent and mesitylene as a solubilizing agent without and with the hydrothermal treatment for 24 h at 288 K, respectively.[48,53] The copolymer−silica complexes were calcined at 823 K for 5 h in air to remove the copolymer template. The specific surface area, micropore volume, total pore volume, and cavity diameter of ASMS-5A are 210 m^2/g, 0.04 cm^3/g, 0.17 cm^3/g, and 13 nm, respectively.[48] ASMS-3A can adsorb NH_3 and CO_2, but not N_2 at their boiling temperatures, while ASMS-5A can adsorb N_2, but not at all isobutane, at their boiling temperatures.[48]

Scanning electron microscopy (SEM) images were recorded on a Hitachi SU8000 field emission scanning electron microscope (FE-SEM), operating at 1 kV. To observe genuine pore structures on the external surface, the sample was observed without any metal coating for SEM.

2. Measurement of Adsorption Isotherms. Prior to the measurements of adsorption isotherms, the materials were outgassed under vacuum at 673 K for 2 h. Adsorption isotherms were measured volumetrically on two types of homemade semiautomated instruments equipped with manometers of full scales of 1000 and 25 000 Torr, respectively. The experimental apparatus and procedures have been described in detail elsewhere.[54] Calculation of adsorption at higher pressures took gas nonideality into consideration on the basis of a Benedict−Webb−Rubin (BWR) equation (CO_2) or a modified BWR equation (N_2, O_2, and CH_4).[55] CO_2 (99.995%) and CH_4 (>99.9%) were obtained from Sumitomo Seika Chemicals, Inc. N_2 (>99.99%), O_2 (>99.5%), and H_2 (>99.99%) were obtained from Air Water, Inc.

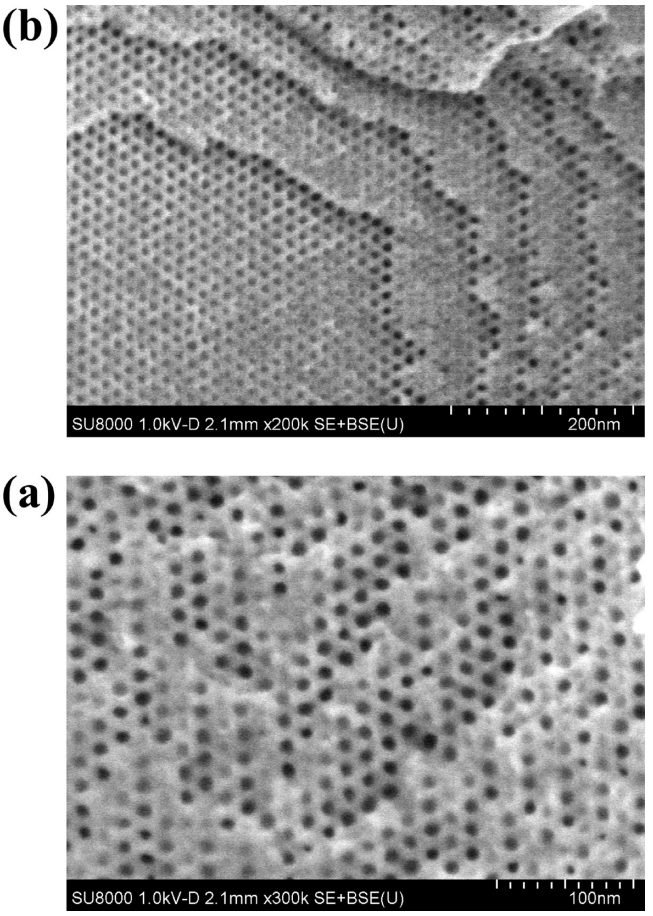

Figure 1. SEM images of ASMS-3A.

III. RESULTS AND DISCUSSION

1. Characterization. From measurements of X-ray diffraction (XRD), transmission electron microscopy (TEM) images, and adsorption isotherms of probe molecules, we have previously shown that ASMS consists of almost spherical cavities arranged in a face-centered-cubic (fcc) array and connected through narrow necks of molecular dimensions.[48] In order to determine further the detailed surface structures of the material, we carried out high-resolution SEM (HR-SEM) observations of ASMS-3A. Figure 1 shows SEM images of the molecular sieve, clearly revealing the well-ordered structure. Although most of the external surfaces are covered with thin silica layers, some part clearly shows two-dimensional hexagonal arrangement of mesopores. This indicates a preferential appearance of the (111) plane in the fcc stacking structure of the spherical cavities on the external surfaces. The image analysis gave the center-to-center distance between the neighboring cavities to be ∼18 nm and thus the unit-cell parameter to be ∼25 nm, being nearly consistent with the value obtained from the XRD pattern.

Apparent dimension of the pores varied with positions over the external surfaces and often the pores were not exposed on the external surfaces. This is consistent with the pore structure of ASMS because a cross-sectional shape of a spherical cavity depends on the position cut and the narrow necks are too small to be observed even by HR-SEM. In addition, terraced structures are often observed (Figure 1b). In most cases, the pores in different terraces are arranged along the same rows. When a height of the

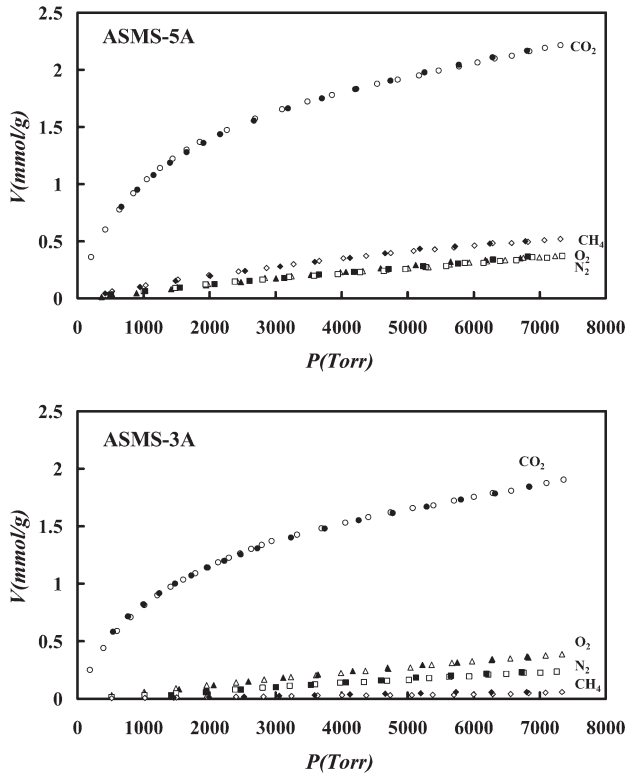

Figure 2. Adsorption−desorption isotherms of CO_2, O_2, N_2, and CH_4 on ASMS-3A and ASMS-5A at 283 K. Open and closed symbols denote adsorption and desorption points, respectively. Solid lines are fits to the dual-site Langmuir−Freundlich model.

terrace is approximately equal to the repeat distance of the (111) close-packed plane, the row of the pores is expected to shift in different terraces. Therefore, it can be considered that in most cases the height of the terrace is smaller than the repeat distance (~14 nm) of the (111) plane. HR-SEM observations confirm the ordered arrangement of the large spherical cavities interconnected through narrow necks where the narrow necks are too small in size to be observed even by HR-SEM. Such narrow necks play an important role in molecular sieving for small molecules such as CO_2 and CH_4.

2. Adsorption and Separation of CO_2/CH_4. The adsorption isotherms of pure CO_2, CH_4, N_2, and O_2 on the dehydrated samples, ASMS-3A and ASMS-5A, were measured up to 10 atm at 283 K. Figure 2 shows the adsorption−desorption isotherms of these gases on the two samples. Adsorption and desorption took place reversibly in several minutes at each point, suggesting excellent regeneration properties of the adsorbents. For ASMS-5A, the amounts of gases adsorbed varied widely, in the sequence $CO_2 \gg CH_4 > N_2 \sim O_2$. This order is compatible with that of the intermolecular interactions in strength, suggesting that a molecular sieving effect does not occur in this material. On the other hand, ASMS-3A exhibited the molecular sieving effect for studied molecules. CH_4 was adsorbed only in a very small amount even at high pressures, and the amount of N_2 adsorbed was smaller than that of O_2. The kinetic diameters of these molecules are in the order $CH_4 \geq N_2 > O_2 > CO_2$.[56] The smaller the kinetic diameter of the molecule, the larger the amount of the gas adsorbed. For ASMS-3A, the exclusion of CH_4 molecules, and possibly N_2 molecules, into the narrow necks was observed. To obtain information about the interactions between adsorbed CO_2 molecules

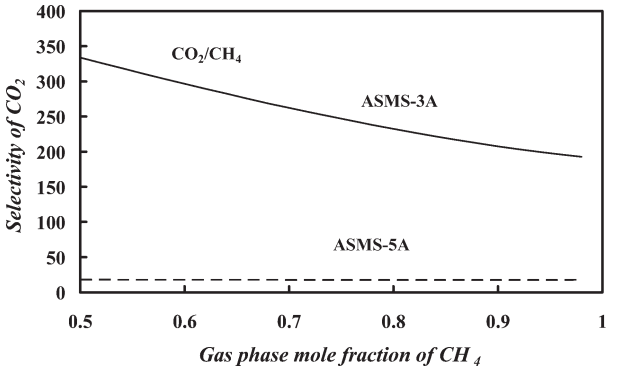

Figure 3. IAST predicted selectivities at different mixture compositions for ASMS-3A and ASMS-5A at 1 atm and 283 K.

and the pore walls, the adsorption isotherms of CO_2 on ASMS-3A were measured at 283, 293, and 303 K up to 1 atm (Figure 1S of the Supporting Information). The isosteric heat of adsorption (~23 kJ/mol) determined from a set of isotherms according to the Clausius−Clapeyron equation did not change appreciably with the adsorbed amount up to the maximum loading (~0.5 mmol/g) reached in this work (Figure 2S of the Supporting Information). This value is comparable to the isosteric heats of adsorption for CO_2 on pure silica zeolites,[11,18] suggesting good regeneration of the adsorbent upon decreasing pressure. Indeed, the adsorption capacity can be restored completely by a brief evacuation of the adsorbent at the measurement temperature.

IAST was used to predict binary mixture adsorption from the experimental pure-gas isotherms.[52] It has been reported that IAST can accurately predict gas mixture adsorption in zeolites,[9,11] carbons,[24,26] and MOF materials.[27,30,39,44] In order to perform the integration required by IAST, the single-component isotherms were fitted by a dual-site Langmuir−Freundlich equation. As can be seen in Figure 2, the equation fits the single-component isotherms very well ($R^2 > 0.998$). Hence, the fitted parameters were used to predict multicomponent adsorption with IAST. Figure 3 shows the IAST-predicted selectivities for CO_2 over CH_4 at different mixture compositions at 1 atm for the two samples. A convenient procedure for PSA process based on CO_2 adsorption could be a process in which the adsorption step takes place at moderate pressures above atmospheric pressure, and desorption must be performed preferentially at atmospheric pressure. The selectivity $S_{A/B}$ in a binary mixture of components A and B is defined as $(x_A/y_A)/(x_B/y_B)$, where x_i and y_i are the mole fractions of component i (i = A, B) in the adsorbed and bulk phases, respectively. For ASMS-3A, the selectivity decreases with an increase of the gas-phase mole fraction of CH_4. At $y_{CH_4} = 0.95$ a typical feed composition for natural gas purification, however, an extraordinary high selectivity of ~200 is still obtained. This is extremely higher than the selectivities reported for zeolites (3−24),[6−9,13,15,18,19] carbon-based adsorbents (2−8),[23,26] and MOFs (2−20),[27,29−31,33,36,37,39−41,43,44,47] at similar conditions. The selectivity for ASMS-5A (~18) did not depend appreciably on the gas-phase mole fraction of CH_4. This selectivity value originates from the separation based on the different adsorption affinities of the two molecules on the pore walls of ASMSs.

It has been reported that some forms of cation-exchanged titanosilicate zeolites can exclude CH_4 while adsorbing substantial amounts of CO_2.[17] However, the materials adsorb strongly CO_2 molecules, thus requiring thermal treatment for regeneration

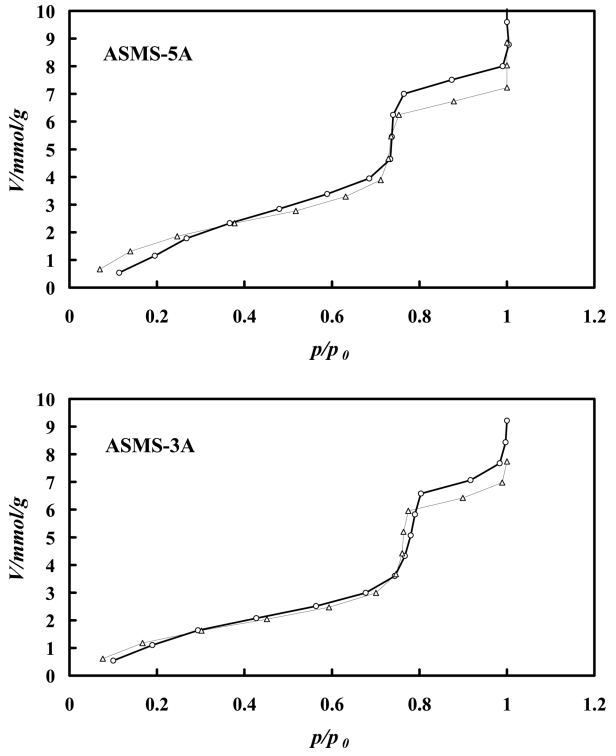

Figure 4. Adsorption isotherms of water on ASMS-3A and ASMS-5A at 283 K. Circles and triangles denote the data points of first and second runs, respectively.

of the adsorbents. Very recently, it has also been reported that a few kinds of MOFs exhibit very large selectivities in CO_2/CH_4 separations.[34,45,46] All these MOFs exhibit stepwise, hysteretic, pressure-dependent adsorption−desorption isotherms for CO_2, indicating that pressure-dependent structure changes occur during adsorption−desorption processes. This suggests that the adsorption and desorption of CO_2 in the materials are not so fast. These features of the adsorption−desorption isotherms might make the application of the adsorbents to the PSA process difficult.

3. Effect of Surface Hydration. Figure 4 shows the adsorption isotherms of water on the two samples at 283 K. For both the samples, the isotherm of the first run is placed slightly below that of the second run in the initial stage of adsorption, whereas in the final stage of adsorption the isotherm of the first run is placed above that of the second run. This suggests that dehydrated surfaces are more hydrophobic than hydrated surfaces and surface hydroxylation takes place gradually with an increase of water vapor pressure during the first run. Capillary condensation of water inside the large cavities of ASMS-3A took place at p/p_0 slightly higher than in ASMS-5A, indicating that the cavities in ASMS-3A are slightly larger than those in ASMS-5A; the average diameter of the cavities in ASMS-5A is ∼13 nm.[48] Previously, the cavity size of ASMS-3A was not determined by a standard nitrogen adsorption method at 77 K because the material did not adsorb appreciably nitrogen at 77 K. It is suggested from a comparison between the adsorption isotherms of water on ASMS-3A and ASMS-5A that the surface area and total pore volume of ASMS-3A are slightly smaller than those of ASMS-5A. The difference in the adsorbed amount of water between the first and second runs at high relative pressures indicates the amount of water strongly

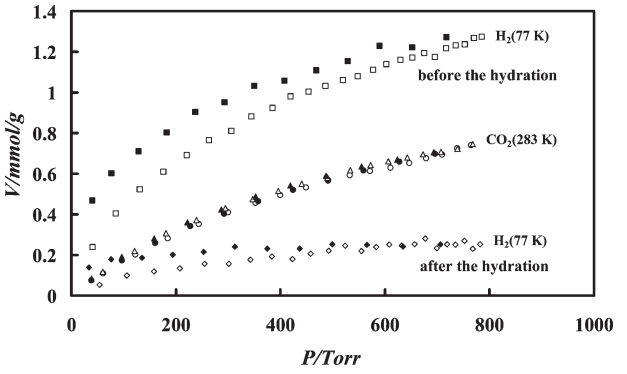

Figure 5. Adsorption−desorption isotherms of CO_2 at 283 K and H_2 at 77 K on ASMS-3A. Circles and triangles denote the data points for CO_2, respectively, before and after the hydration of the substrate. Open and closed symbols denote adsorption and desorption points, respectively.

adsorbed on the surfaces, that is, the amount of surface hydroxyls formed on the pore walls. It is inferred from the surface area of the material (210 m^2/g) and the amount (0.78 mmol/g) of water strongly adsorbed on the surfaces that the density of hydroxyl groups formed on the pore walls of ASMS-5A by surface hydroxylation is ∼4.4 OH/nm^2. The amount (∼0.6 mmol/g) of water strongly adsorbed on ASMS-3A suggests the smaller density of hydroxyl groups formed on the pore walls compared to ASMS-5A. Figure 5 shows the adsorption−desorption isotherms of CO_2 at 283 K and H_2 at 77 K on ASMS-3A measured before and after surface hydration. On surface hydration, the amount of H_2 adsorbed at 77 K decreased considerably. This indicates narrowing of the necks interconnecting the large cavities by surface hydroxylation of the pore walls surrounding the necks. In zeolites of low Si/Al ratios, it is well-known that the amount of CO_2 adsorbed decreases significantly with surface hydration.[57] For ASMS-3A, however, the amount of CO_2 adsorbed at 283 K did not decrease at all with surface hydration. This implies that a prewater treatment is probably not required prior to the separation process for this adsorbent. In addition, the adsorbent does not require thermal treatment for removal of surface hydroxyls prior to use. The kinetic diameter of CO_2 is slightly larger than that of H_2, and consequently by far the most important factor in resulting in the different effect of surface hydration is the higher temperature of measurement. This strongly suggests the diffusional limitations of adsorbate molecules through the narrow necks into the large cavities beyond at low temperature. Hysteresis between adsorption and desorption branches of H_2 at 77 K is also in line with this idea.

For ASMS-3A, the exclusion of CH_4 molecules due to their dimensions into the narrow necks and preferential adsorption of CO_2 with the smaller kinetic diameter was observed at 283 K, indicating that the diameter of the narrow necks in the material is in the narrow range (∼0.33−0.38 nm) between the kinetic diameters of the two molecules. Such an entrance size corresponds to the free dimensions of rings composed of 8-SiO_4 tetrahedra in crystalline zeolites.[58] In ASMS-3A, the narrow necks would be cylindrical pores that are composed of the 8-membered rings, some fraction of which are deficient in oxygen atoms. Surface hydration will result in formation of surface hydroxyls on the defect sites of the cylindrical pores because the 8-membered rings of crystalline zeolites do not adsorb H_2O molecules dissociatively. NMR studies have shown that the librational motions of surface hydroxyls on silica gel are almost frozen out at 77 K, and

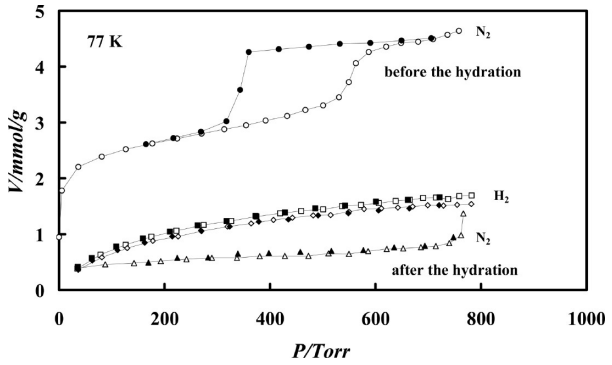

Figure 6. Adsorption−desorption isotherms of N_2 and H_2 at 77 K on ASMS-5A. Squares and diamonds denote the data points for H_2, respectively, before and after the hydration of the substrate. Open and closed symbols denote adsorption and desorption points, respectively.

the librational amplitudes increase with increasing temperature.[59] Therefore, it is plausible to imagine that the silanols executing librational motions about the internuclear Si−O axes do not block the narrow necks for passage of CO_2 molecules.

The diameter of the narrow necks in ASMS-5A is in the range of 0.37−0.53 nm.[48] Therefore, CH_4 molecules can be diffused through the narrow necks into the large cavities beyond. Figure 6 shows the adsorption−desorption isotherms of N_2 and H_2 at 77 K on ASMS-5A measured before and after surface hydration. The amount of N_2 adsorbed at 77 K decreased significantly with surface hydration, while that of H_2 decreased only slightly. The adsorption capacity of N_2 at 77 K was gradually restored by subsequent treatment of ASMS-5A in vacuo with increasing temperature (Figure 3S of the Supporting Information). This clearly indicates that the entrance size of the large cavities is slightly reduced by the formation of surface hydroxyls on the pore walls of the necks to the extent that the passage of N_2 molecules through the narrow necks of molecular dimensions is almost completely blocked but blocking for H_2 molecules with the smaller kinetic diameter is limited.

In conclusion, all these results suggest that ASMS-3A is a promising candidate for the separation and purification of CO_2 from various CO_2/CH_4 mixtures such as natural gas and landfill gas by the PSA process.

■ ASSOCIATED CONTENT

Supporting Information. Adsorption−desorption isotherms of CO_2 at 283, 293, and 303 K on ASMS-3A, isosteric heats of adsorption determined from a set of isotherms, and adsorption−desorption isotherms of N_2 at 77 K on ASMS-5A dehydrated at different temperatures. This material is available free of charge via Internet at http://pubs.acs.org.

■ ACKNOWLEDGMENT

We express our sincere thanks to K. Ito and S. Takeuchi of Hitachi High-Technologies Corporation for observations of the HR-SEM images for ASMS-3A. This work was supported by matching fund subsidy for private universities from MEXT (Ministry of Education, Culture, Sports, Science and Technology).

■ REFERENCES

(1) Koros, W. J.; Mahajan, R. *J. Membr. Sci.* **2000**, *175*, 181.
(2) Cavenati, S.; Grande, C. A.; Rodrigues, A. E. *Energy Fuels* **2006**, *20*, 2648.
(3) Sircar, S. *Ind. Eng. Chem. Res.* **2006**, *45*, 5435.
(4) Sircar, S. *Ind. Eng. Chem. Res.* **2002**, *41*, 1389.
(5) Sun, M. S.; Shah, D. B.; Xu, H. H.; Talu, O. *J. Phys. Chem. B* **1998**, *102*, 1466.
(6) Cavenati, S.; Grande, C. A.; Rodrigues, A. E. *J. Chem. Eng. Data* **2004**, *49*, 1095.
(7) Delgado, J. A.; Uguina, M. A.; Gómez, J. M.; Ortega, L. *Sep. Purif. Technol.* **2006**, *48*, 223.
(8) Leyssale, J.−M.; Papadopoulos, G. K.; Theodorou, D. N. *J. Phys. Chem. B* **2006**, *110*, 22742.
(9) Babarao, R.; Hu, Z.; Jiang, J.; Chempath, S.; Sandler, S. I. *Langmuir* **2007**, *23*, 659.
(10) Li, P.; Tezel, F. H. *Microporous Mesoporous Mater.* **2007**, *98*, 94.
(11) Himeno, S.; Tomita, T.; Suzuki, K.; Yoshida, S. *Microporous Mesoporous Mater.* **2007**, *98*, 62.
(12) Delgado, J. A.; Uguina, M. A.; Sotelo, J. L.; Ruíz, B.; Rosário, M.; J. *Natural Gas Chem.* **2007**, *16*, 235.
(13) Venna, S. R.; Carreon, M. A. *J. Phys. Chem. B* **2008**, *112*, 16261.
(14) Pillai, R. S.; Peter, S. A.; Jasra, R. V. *Microporous Mesoporous Mater.* **2008**, *113*, 268.
(15) Ghoufi, A.; Gaberova, L.; Rouquerol, J.; Vincent, D.; Llewellyn, P. L.; Maurin, G. *Microporous Mesoporous Mater.* **2009**, *119*, 117.
(16) Zhao, X.-X.; Xu, X.-L.; Sun, L.-B.; Zhang, L.-L.; Liu, X. Q. *Energy Fuels* **2009**, *23*, 1534.
(17) Anson, A.; Lin, C. C. H.; Kuznicki, S. M.; Sawada, J. A. *Chem. Eng. Sci.* **2009**, *64*, 3683.
(18) Palomino, M.; Corma, A.; Rey, F.; Valencia, S. *Langmuir* **2010**, *26*, 1910.
(19) Huang, Z.; Xu, L.; Li, J.-H.; Guo, G.-M.; Wang, Y. *J. Chem. Eng. Data* **2010**, *55*, 2123.
(20) Kapoor, A.; Yang, R. T. *Chem. Eng. Sci.* **1989**, *44*, 1723.
(21) Sircar, S.; Golden, T. C.; Rao, M. B. *Carbon* **1996**, *34*, 1.
(22) Qinglin, H.; Farooq, S.; Karimi, I. A. *Langmuir* **2003**, *19*, 5722.
(23) Peng, X.; Wang, W.; Xue, R.; Shen, Z. *AIChE J.* **2006**, *52*, 994.
(24) Goetz, V.; Pupier, O.; Guillot, A. *Adsorption* **2006**, *12*, 55.
(25) Watson, G.; May, E. F.; Graham, B. F.; Trebble, M. A.; Trengove, R. D.; Chan, K. I. J. *Chem. Eng. Data* **2009**, *54*, 2701.
(26) Shen, Y.; Bai, J. *Chem. Commun.* **2010**, *46*, 1308.
(27) Yang, Q.; Zhang, C. *J. Phys. Chem. B* **2006**, *110*, 17776.
(28) Llewellyn, P. L.; Bourrelly, S.; Serre, C.; Vimont, A.; Daturi, M.; Hamon, L.; Weireld, G. D.; Chang, J.-S.; Hong, D.-Y.; Hwang, Y. K.; Jhung, S. H.; Férey, G. *Langmuir* **2008**, *24*, 7245.
(29) Wang, B.; Côté, A. P.; Furukawa, H.; O'Keeffe, M.; Yaghi, O. M. *Nature* **2008**, *453*, 207.
(30) Bae, Y.-S.; Mulfort, K. L.; Frost, H.; Ryan, P.; Punnathanam, S.; Broadbelt, L. J.; Hupp, J. T.; Snurr, R. Q. *Langmuir* **2008**, *24*, 8592.
(31) Liang, Z.; Marshall, M.; Chaffee, A. L. *Energy Fuels* **2009**, *23*, 2785.
(32) Dietzel, P. D. C.; Besikiotis, V.; Blom, R. *J. Mater. Chem.* **2009**, *19*, 7362.
(33) Finsy, V.; Ma, L.; Alaerts, L.; De Vos, D. E.; Baron, G. V.; Denayer, J. F. M. *Microporous Mesoporous Mater.* **2009**, *120*, 221.
(34) Couck, S.; Denayer, J. F. M.; Baron, G. V.; Rémy, T.; Gascon, J.; Kapteijn, F. *J. Am. Chem. Soc.* **2009**, *131*, 6326.
(35) Bae, Y.-S.; Dubbeldam, D.; Nelson, A.; Walton, K. S.; Hupp, J. T.; Snurr, R. Q. *Chem. Mater.* **2009**, *21*, 4768.
(36) Banerjee, R.; Furukawa, H.; Britt, D.; Knobler, C.; O'Keeffe, M.; Yaghi, O. M. *J. Am. Chem. Soc.* **2009**, *131*, 3875.
(37) Yazaydin, A. Ö.; Benin, A. I.; Faheem, S. A.; Jakubczak, P.; Low, J. J.; Willis, R. R.; Snurr, R. Q. *Chem. Mater.* **2009**, *21*, 1425.
(38) Miller, S. R.; Wright, P. A.; Devic, T.; Serre, C.; Férey, G.; Llewellyn, P. L.; Denoyel, R.; Gaberova, L.; Filinchuk, Y. *Langmuir* **2009**, *25*, 3618.

(39) Farha, O. K.; Spokoyny, A. M.; Hauser, B. G.; Bae, Y.-S.; Brown, S. E.; Snurr, R. Q.; Mirkin, C. A.; Hupp, J. T. *Chem. Mater.* **2009**, *21*, 3033.
(40) Hamon, L.; Llewellyn, P. L.; Devic, T.; Ghoufi, A.; Clet, G.; Guillerm, V.; Pirngruber, G. D.; Maurin, G.; Serre, C.; Driver, G.; van Beek, W.; Jolimaître, E.; Vimont, A.; Daturi, M.; Férey, G. *J. Am. Chem. Soc.* **2009**, *131*, 17490.
(41) Liang, Z.; Marshall, M.; Chaffee, A. L. *Microporous Mesoporous Mater.* **2010**, *132*, 305.
(42) Zhang, S.-M.; Chang, Z.; Hu, T.-L.; Bu, X.-H. *Inorg. Chem.* **2010**, *49*, 11581.
(43) Chen, Y. F.; Lee, J. Y.; Babarao, R.; Li, J.; Jiang, J. W. *J. Phys. Chem. C* **2010**, *114*, 6602.
(44) Liu, B.; Smit, B. *J. Phys. Chem. C* **2010**, *114*, 8515.
(45) Inubushi, Y.; Horike, S.; Fukushima, T.; Akiyama, G.; Matsuda, R.; Kitagawa, S. *Chem. Commun.* **2010**, *46*, 9229.
(46) Zhang, J.; Wu, H.; Emge, T. J.; Li, J. *Chem. Commun.* **2010**, *46*, 9152.
(47) Bao, Z.; Yu, L.; Ren, Q.; Lu, X.; Deng, S. *J. Colloid Interface Sci.* **2011**, *353*, 549.
(48) Morishige, K.; Yasuki, T. *J. Phys. Chem. C* **2010**, *114*, 10910.
(49) Sakamoto, Y.; Kaneda, M.; Terasaki, O.; Zhao, D. Y.; Kim, J. M.; Stucky, G. D.; Shin, H. J.; Ryoo, R. *Nature* **2000**, *408*, 449.
(50) Morishige, K.; Kanzaki, Y. *J. Phys. Chem. C* **2009**, *113*, 14927.
(51) Morishige, K.; Yoshida, K. *J. Phys. Chem. C* **2010**, *114*, 7095.
(52) Myers, A. L.; Prausnitz, J. M. *AIChE J.* **1965**, *11*, 121.
(53) Yu, T.; Zhang, H.; Yan, X.; Chen, Z.; Zou, X.; Oleynikov, P.; Zhao, D. *J. Phys. Chem. B* **2006**, *110*, 21467.
(54) Morishige, K.; Ito, M. J. *Chem. Phys.* **2002**, *117*, 8036.
(55) *Kagaku-Binran*, edited by the Chemical Society of Japan; Maruzen: Tokyo, 1993; Vol. 2, p 115.
(56) Li, J.-R.; Kuppler, R. J.; Zhou, H.-C. *Chem. Soc. Rev.* **2009**, *38*, 1477.
(57) Brandani, F.; Ruthven, D. M. *Ind. Eng. Chem. Res.* **2004**, *43*, 8339.
(58) Barrer, R. M.; Kerr, I. S. *Trans. Faraday Soc.* **1959**, *55*, 1915.
(59) Kobayashi, T.; DiVerdi, J. A.; Maciel, G. E. *J. Phys. Chem. C* **2008**, *112*, 4315.